Lee *Fisheries and Aquatic Sciences* (2016) 19:8
DOI 10.1186/s41240-016-0010-3

Fisheries and Aquatic Sciences

RESEARCH ARTICLE Open Access

The influence of cuttlebone on the target strength of live golden cuttlefish (*Sepia esculenta*) at 70 and 120 kHz

Daejae Lee

Abstract

To quantitatively estimate the influence of cuttlebone on the target strength (*TS*) of golden cuttlefish, the cuttlebone was carefully extracted from 19 live cuttlefish caught using traps in the inshore waters around Geojedo, Korea, in early May 2010 and the *TS* was measured using split-beam echosounders (Simrad ES60 and EY500). The *TS-length* relationships for the cuttlefish (before the extraction of cuttlebone, Fish Aquat Sci. 17:361–7, 2014) and the corresponding cuttlebone were compared. The cuttlebone length (L_b) ranged from 151 to 195 mm (mean $L_b = 168.3$ mm) and the mass (W_b) ranged from 29.3 to 53.2 g (mean $W_b = 38.8$ g). The mean *TS* values at 70 and 120 kHz were −33.60 dB (std = 1.12 dB) and −32.24 dB (std = 1.87 dB), respectively. The mean *TS* values of cuttlebone were 0.19 dB and 0.04 dB lower than those of cuttlefish at 70 and 120 kHz, respectively. For 70 and 120 kHz combined, the mean *TS* value of cuttlebone was −32.87 dB, 0.11 dB lower than that of cuttlefish (−32.76 dB). On the other hand, the mean *TS* value of cuttlebone predicted by the regression ($TS_b = 24.86 \log_{10} L_b - 4.86 \log_{10} \lambda - 22.58$, $r^2 = 0.85$, $N = 38$, $P < 0.01$) was −33.10 dB, 0.04 dB lower than that of cuttlefish predicted by the regression ($TS_c = 24.62 \log_{10} L_c - 4.62 \log_{10} \lambda - 22.64$, $r^2 = 0.85$, $N = 38$, $P < 0.01$). That is, the contribution of cuttlebone to the cuttlefish *TS* determined by the measured results was slightly greater than that by the predicted results. These results suggest that cuttlebone is responsible for the *TS* of cuttlefish, and the contribution is estimated to be at least 99 % of the total echo strength.

Keywords: *Sepia esculenta* Target strength, Influence of cuttlebone, Tilt angle, Length dependence

Background

Most aquatic animals, such as swimbladder fish and cuttlefish, maintain their depth in the sea by adjusting their average density to equal that of seawater using gas-filled organs that serve as a buoyancy tank (Denton and Gilpin-Brown 1961; Denton et al. 1961; Denton and Taylor 1964). These aquatic animals use essentially the same mechanism in their swimbladders and cuttlebones to achieve the buoyancy control needed to minimize energy consumption (Midtvedt et al. 2007). If the body density is higher than the surrounding water, the animal sinks. Similarly, aquatic animals of lower density float towards the surface. As long as the aquatic animal is not moving, this task is fairly simple, but aquatic animals move and as soon as the animal ascends or descends, the hydrostatic pressure changes. In swimbladder fish, to compensate for this, gas must be rapidly secreted into the swimbladder while descending and removed while ascending (Denton and Gilpin-Brown 1961; Denton et al. 1961; Denton and Taylor 1964; Fnney et al. 2006). However, in cuttlefish, such problems of pressure change are avoided by enclosing the gas inside an incompressible chamber within the cuttlebone, the volume of which is unaffected by depth, and so cuttlefish maintain neutral buoyancy almost independent of depth (Sherrard 2000). Thus, the buoyancy mechanisms used by cuttlefish and swimbladder fish differ. The cuttlebone of cuttlefish comprises ~9 % of total body volume, but the swimbladder of fish only 4–6 % of total body volume (Denton and Gilpin-Brown 1961; Denton et al. 1961; Denton and Taylor 1964; Webber et al. 2000; Horne 2008; Sunardi et al. 2008). Foote et al. (Foote 1980a, 1980b, 1985; Foote and Ona 1985) indicated that the swimbladder is responsible for more than 90 % of the reflected sound energy from a fish. These facts suggest that the

Correspondence: daejael@pknu.ac.kr
Division of Marine Production System Management, Pukyong National University, Busan 48513, Korea

© 2016 Lee. **Open Access** This article is distributed under the terms of the Creative Commons Attribution 4.0 International License (http://creativecommons.org/licenses/by/4.0/), which permits unrestricted use, distribution, and reproduction in any medium, provided you give appropriate credit to the original author(s) and the source, provide a link to the Creative Commons license, and indicate if changes were made. The Creative Commons Public Domain Dedication waiver (http://creativecommons.org/publicdomain/zero/1.0/) applies to the data made available in this article, unless otherwise stated.

contribution of cuttlebone to the *TS* of cuttlefish may be larger than that of the swimbladder to the *TS* of fish, if the volume of cuttlebone does not change with depth. Other than our earlier study (Lee and Demer 2014), there has been no systematic attempt to determine the relationship between the *TS* and size of cuttlefish, especially the importance of cuttlebone to cuttlefish *TS*.

The objective of this study was to estimate the influence of cuttlebone on the *TS* of golden cuttlefish (*Sepia esculenta*), by comparing the *TS-L* relationships for cuttlebone and cuttlefish at 70 and 120 kHz.

Methods

Echosounders and calibrations

The acoustic and mechanical system for measuring the *TS* of cuttlebone is shown in Fig. 1 (Lee and Demer 2014). It comprised two split-beam echosounders (ES60 and EY500, Simrad, Norway) operating at 70 and 120 kHz, two split-beam transducers (half-power beamwidths = 11° and 7.1°, respectively) and a DC servomotor system (motor: BG90, Sung Shin, Korea; driver: KDC248H, KScontrol, Korea) to control the tilt angles of the cuttlebone during each acoustic transmission. A water-cooling system maintained the seawater at a temperature $T = 18.0$ °C (confirmed by measurements before and near the end of the experiment). The two transducers were mounted adjacently facing sidewards, with the center of their faces at approximately 56 cm below the water surface.

Before and near the end of the experiments, the 70 and 120 kHz echosounders were calibrated using copper spheres of 32.1 and 23.0 mm diameter, respectively. The *TS* measurements were corrected for these calibrated offsets (−0.3 dB at 70 kHz and 0.5 dB at 120 kHz).

The experiment was conducted under the guidelines of Animal Ethics Committee Regulations, No. 554 issued from Pukyong National University, Busan, Korea. Nineteen cuttlebones directly extracted from 19 of the 23 live cuttlefish individuals (with the exception of four broken cuttlebones) tested in our earlier study (Lee and Demer 2014) were used as specimens for the *TS* measurements. Each cuttlebone was carefully extracted from each live cuttlefish specimen in sea water just before the experiment, and then immediately moved to a small tank filled with seawater at 18 °C.

To avoid variations in the acoustic and physical properties of the extracted cuttlebone with time, especially due to changes in shape, structure, chamber space and density, the cuttlebone *TS* measurement was rapidly performed under almost identical conditions, but in another acrylic salt-water tank, following measurement of the *TS* of live cuttlefish.

Before each set of measurements, the specimen was carefully suspended into the overlapping sound beams, avoiding the introduction of air bubbles. The tilt angle

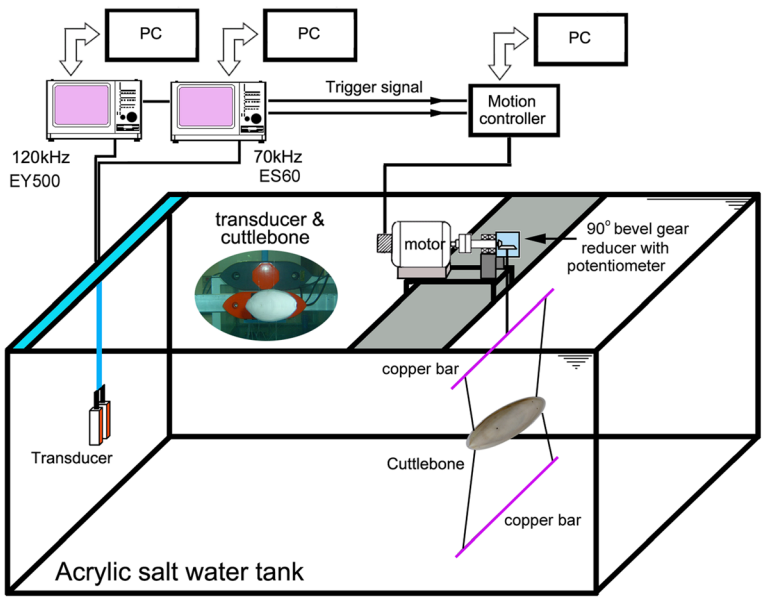

Fig. 1 Diagram of the acoustic-mechanical apparatus used to measure cuttlebone target strength (*TS*) versus length (L_b), and tilt angle (θ). The apparatus comprise: a rectangular (1.2 width x 1.8 length x 1.2 m height), acrylic, saltwater tank; 70 and 120 kHz echosounders (Simrad ES60 and EY500, respectively); two split-beam transducers (Simrad ES70-11 and ES120-7 F, respectively); and a DC servo-motor system for controlling the tilt angle of cuttlebone. The cuttlebone was slowly rotated for the angle range of −90° (head-down orientation) to 90° (head-up orientation) at a fixed speed of 0.167 rpm and stably maintained by tying monofilament lines between both ends of cuttlebone and two horizontal bars for suspending

of the cuttlebone was controlled using four monofilament lines (0.2 mm diameter), each tied to the anterior (head) and posterior (spine) parts of the cuttlebone, at both ends of an upper copper bar connected to the rotating axis of a DC servomotor system, and at both ends of a lower copper bar acting as a balancing weight (Fig. 1). The tilt angle was measured using a precision potentiometer (CP50, Sakae Tsushin Kogyo, Japan) connected to the axis of a 90° bevel gear reducer (ratio 240:1). The rotation speed of the cuttlebone was controlled by changing the input voltage of the DC servomotor system.

The definition of tilt angle for cuttlebone is shown in Fig. 2. The precise dorsal aspect of cuttlebone relative to the axis of the transducer was defined as a tilt angle of 0°, and the head up and down orientations relative to the center line of the cuttlebone were defined as positive θ and negative θ values, respectively.

In each case, the range between the transducers and the cuttlebone was approximately 1.2 m. The far-field ranges for the 70 and 120 kHz transducers (diameter d =13.5 and 12.9 cm) were ~0.47 and ~0.68 m (Lee 2006; Foote 2012), respectively. During the calibrations and the *TS* measurements, the 70 and 120 kHz echosounders transmitted 300 and 60 W pulses with durations of 256 μs and 300 μs every 0.2 s, and received the echoes using 6.2 and 12 kHz receiver bandwidths, respectively. The experiments in all cases were conducted using the same pulse duration, transmit power, pulse repetition interval and bandwidth used during the *TS* measurement of the calibration sphere. To avoid crosstalk, the measurements at 70 and 120 kHz were taken sequentially. When the trigger pulse of the echosounder was transferred to a PC-based motor controller (Comi-SD501, Comizoa, Korea) and signal processor (Comi-LX102, Comizoa, Korea), the *TS* measurement for the cuttlebone rotating at a fixed speed of 0.167 rpm, from the head-down orientation (−90°) to the head-up orientation (+90°), was conducted continuously. The output voltage of the precision potentiometer corresponding to the tilt angle and the echo data were recorded simultaneously and later processed to estimate the relationship between *TS* and tilt angle (θ) during each transmission. The echo data, logged by the echosounders, were post-processed using commercial software (Echoview V3.3, Sonar Data, Australia; EP500 v. 5.2, Simrad, Norway).

Specimens and measurement of target strength

The biological and morphological characteristics of 19 specimens of cuttlebone and the corresponding live cuttlefish (Lee and Demer 2014) used in the *TS* experiments are shown in Table 1. These characteristics—such as length, weight, width and thickness—were measured following completion of the acoustic experiments. Mantle length (L_c) and body mass (W_c) for cuttlefish ranged from 156 to 203 mm (mean L_c = 173.9; deviation (std) = 13.10 mm) and 335–720 g (mean W_c = 527.4; std = 104.4 g), respectively. The length (L_b), weight (W_b), width (W_d) and thickness (T_h) of cuttlebone ranged from 151 to 195 mm (mean L_b = 168.3; std = 12.56 mm), 29.3–53.2 g (mean W_b = 38.8; std = 7.23 g), 55–69 mm (mean W_d = 62.4; std = 4.10 mm), and 13.6–18.0 mm (mean T_h = 15.7; std = 1.24 mm), respectively.

The mean tilt angles (<θ>) with standard deviations (S_θ) measured for 19 live cuttlefish at 70 and 120 kHz in our earlier study (Lee and Demer 2014) are shown in Table 2. The *TS* and θ for these live cuttlefish were measured simultaneously using a split-beam echo sounder and a CCTV camera system, respectively and the (<θ>) and S_θ values were used in estimating the tilt-averaged *TS* from the *TS* functions of the corresponding cuttlebone.

In the 70 kHz experiments, the mean tilt angles of 19 live cuttlefish varied from −3.51° to −1.05° (mean −2.31°,

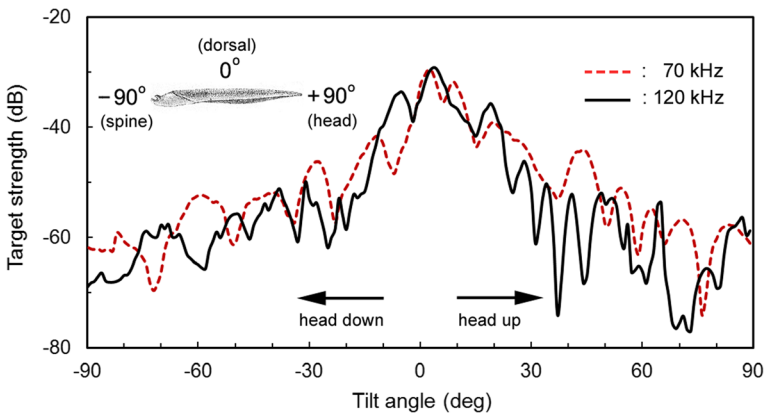

Fig. 2 Comparison of the *TS* functions for cuttlebone (L_b =15.2 cm, W_b =29.3 g) measured as a function of tilt angle at 70 (*dash line*) and 120 kHz (*solid line*). The precise dorsal-aspect orientation is defined by the angle 0°, and the precise head-down and head-up orientations are defined by angles −90° and 90°, respectively

Table 1 Biological characteristics of the corresponding cuttlebone and the body of 19 live cuttlefishes used in the *TS* measurements

Specimen No.	Cuttlefish		Cuttlebone			
	Length[a] (mm)	Weight (g)	Length (mm)	Weight (g)	Width (mm)	Thickness (mm)
1	194	550	185	41.2	63.0	14.8
2	176	435	172	41.6	61.4	15.6
3	165	520	159	31.9	68.0	14.3
4	178	510	173	39.0	66.7	16.8
5	182	643	175	47.9	64.4	16.4
6	174	565	169	33.4	61.0	15.1
7	164	370	155	37.4	58.1	18.0
8	176	512	171	45.3	68.0	16.4
9	158	335	152	29.3	59.8	14.9
10	203	720	195	47.9	66.0	17.2
11	161	475	158	31.3	55.0	13.6
12	156	450	151	31.8	59.0	15.0
13	166	420	161	33.6	62.9	15.5
14	172	530	166	35.9	63.2	15.3
15	177	645	173	48.8	62.0	16.6
16	176	675	173	42.4	59.3	17.8
17	197	645	191	53.2	69.0	16.4
18	160	475	155	30.1	55.0	13.9
19	169	545	163	35.1	63.0	15.5
mean	173.9	527.4	168.3	38.8	62.4	15.7

[a] The length of cuttlefish is a dorsal mantle length

head-down), while the standard deviation varied from 2.32° to 12.64° (mean 6.56°). At 120 kHz, the mean tilt angles varied from −5.11° to −0.73° (mean −3.15°), while the standard deviation varied from 2.33° to 6.86° (mean 4.74°).

Target strength models

To compare the *TS* of cuttlebone with that of live cuttlefish, two *TS* values, such as the maximum *TS* (TS_m) and the tilt-averaged *TS* ($<TS_b>$) in the dorsal-aspect orientation of the cuttlebone, were estimated. First, the TS_m was obtained directly from the measured *TS* functions. Next, the $< TS_b >$ was calculated by using the probability density function $f(\theta)$ of tilt angle θ, with mean θ ($<\theta>$) and standard deviation S_θ, according to Eqs. (1) and (2) (Foote 1980a, 1980b; Pena and Foote 2008):

$$< \sigma > \; = \int \sigma(\theta) f(\theta)\, d\theta \tag{1}$$

$$< TS_b > \; = \; 10 \log(< \sigma > /4\pi) \tag{2}$$

where θ is the tilt angle defined as the angle made by the cuttlebone centerline with the horizontal, $\sigma(\theta)$ is the backscattering cross section of tilt angle θ and the tilt-angle distribution $f(\theta)$ was assumed to be a truncated normal distribution function. For each cuttlebone, the $< TS_b >$ was computed over the range $< \theta > -3\ S_\theta$ to $< \theta > +3\ S_\theta$ using the mean tilt angle ($<\theta>$) with standard deviation (S_θ) indicated in Table 2.

Each dataset of the mean *TS* of cuttlebone and cuttlefish obtained for 19 specimens at 70 and 120 kHz was regressed on specimen length L and wavelength λ according to the empirical equation. First, to establish empirical single-frequency relationships between the $< TS >$ and the corresponding L, the dataset for each frequency was independently fit, in the least-squares sense, to (Benoit-Bird et al. 2008; Conti and Demer. 2003; Demer and Martin 1995; Foote 1987; Goddard and Welsby 1986; Imaizumi et al. 2008; Kang et al. 2005; Sawada et al. 2011):

$$TS = m \log_{10} L + b \tag{3}$$

where L is the specimen length (cm), m is the slope of the regression line, and b is the intercept of the regression line on the *TS* axis.

Next, the datasets from both frequencies were combined to obtain a relationship for a wider range of specimen lengths (L) and wavelengths (λ):

Table 2 Mean tilt angles (<θ>) with standard deviations (S_θ) used in estimating the mean *TS* of cuttlebone at 70 and 120 kHz (Lee and Demer 2014). The *TS* and θ for live cuttlefish were simultaneously measured by a split-beam echo sounder and a CCTV system, respectively

Specimen No.	70 kHz			120 kHz		
	M. tilt angle (deg)	Standard dev. (deg)	*N*	M. tilt angle (deg)	Standard dev. (deg)	*N*
1	−3.08	12.64	14	−3.15	3.27	16
2	−1.71	6.21	15	−3.01	5.46	15
3	−2.96	7.39	15	−4.77	6.23	15
4	−3.01	9.19	15	−2.01	2.93	15
5	−2.29	2.32	15	−2.29	2.33	15
6	−1.93	3.83	15	−3.03	4.99	15
7	−1.75	5.41	15	−4.23	6.45	15
8	−2.71	9.61	14	−4.87	3.91	14
9	−2.71	5.99	15	−3.25	5.49	15
10	−1.17	3.37	15	−5.11	4.10	15
11	−2.39	5.28	15	−4.61	5.76	15
12	−1.05	6.76	15	−2.37	5.67	15
13	−3.51	8.52	15	−4.55	4.46	15
14	−1.21	3.63	15	−0.73	5.24	15
15	−1.91	6.84	15	−2.39	3.03	15
16	−1.71	6.44	15	−1.43	5.56	15
17	−3.27	6.53	15	−2.77	6.86	15
18	−2.97	6.17	15	−3.07	4.71	15
19	−2.61	8.56	15	−2.13	3.68	15
mean	−2.31	6.56		−3.15	4.74	

$$TS = a\log_{10}L + b\log_{10}\lambda + c \quad (4)$$

where L is the specimen length (m), λ is the acoustic wavelength (m), and a, b, c are the fitted coefficients (Love 1969, 1971; McClatchie et al. 1996, 2003).

The mean TS (<TS_c>) of live cuttlefish was derived from the results of TS measurements of the same specimen listed in Table 1 and described fully in our earlier study (Lee and Demer 2014). The influence of cuttlebone on the cuttlefish TS (<TS_c>) was analyzed by estimating the difference between these mean TS values and by comparing the *TS-length* relationships for the corresponding cuttlebone and the cuttlefish at 70 and 120 kHz.

Results

The < TS_b > of 19 cuttlebones were plotted separately for 70 and 120 kHz versus cuttlebone length L_b, overlaid on the regressions of Eq. (3) (Figs. 3 and 4).

At 70 kHz,

$$TS = 22.03\log_{10}(L_b \text{ in cm}) - 60.72, \quad (5)$$
$$\left(r^2 = 0.40, N = 19, P < 0.01\right).$$

At 120 kHz,

$$TS = 28.53\log_{10}(L_b \text{ in cm}) - 67.55 \quad (6)$$
$$\left(r^2 = 0.24, N = 19, P < 0.05\right).$$

The mean < TS_b > at 70 kHz was −33.60 dB, 1.36 dB lower than that at 120 kHz (−32.24 dB). The mean < TS_b > at 70 kHz was 0.30 dB higher than that indicated by Eq. (5) and the mean < TS_b > at 120 kHz was 0.33 dB higher

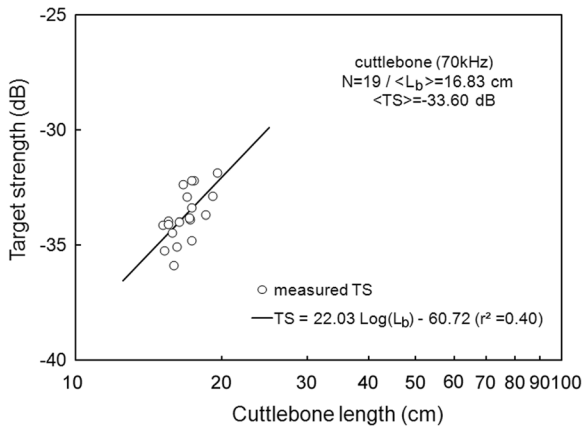

Fig. 3 Relationship between mean *TS* (<TS_b>) and cuttlebone length (L_b) at 70 kHz for 19 cuttlebones extracted from cuttlefish caught during the spawning season in the southwest waters of Korea

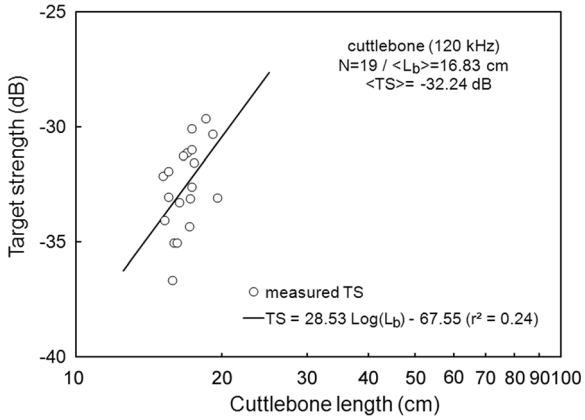

Fig. 4 Relationship between mean *TS* (<TS_b>) and cuttlebone length (L_b) at 120 kHz for 19 cuttlebones extracted from cuttlefish caught during the spawning season in the southwest waters of Korea

than that indicated by Eq. (6). The difference between the slopes of the regressions for these frequencies was 6.5, and the intercept at 70 kHz was 6.83 dB higher than that at 120 kHz (Eqs. 5 and 6).

For 70 and 120 kHz combined, the 38 measurements of < TS_b > and TS_m were transformed to mean scattering cross-sectional areas (σ; m^2) and σ^2/λ was plotted versus L/λ (Fig. 5). In Fig. 5, the TS_m in the dorsal-aspect orientation of cuttlebone was derived by simple extraction from the *TS* function measured as a function of tilt angle. The mean *TS* (<TS_c>) of live cuttlefish was obtained from the results of *TS* measurements of the

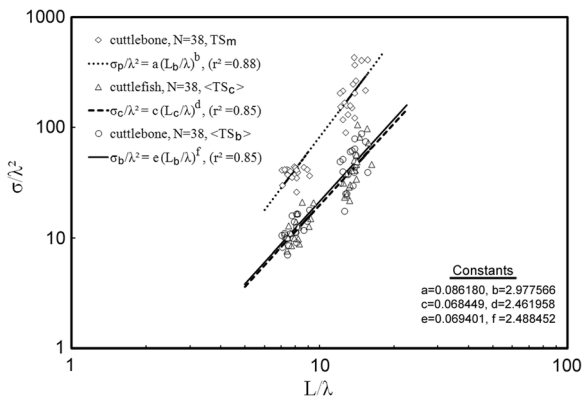

Fig. 5 Comparison of the relationships between σ/λ^2 and L/λ for each dataset of cuttlebone and cuttlefish (Lee and Demer 2014) obtained by combining 120 kHz data (Fig. 4) with 70 kHz data (Fig. 3), where σ_p, σ_b and σ_c are scattering cross-sectional areas (m^2) corresponding to the maximum *TS* (TS_m) and the mean *TS* (<TS_b>) of cuttlebone, and the mean *TS* (<TS_c>) of cuttlefish, respectively. L_b and L_c is the lengths (m) of cuttlebone and cuttlefish, respectively and λ is the acoustic wavelength (m). The *TS-L* relationships for cuttlebone and cuttlefish was converted from the relationships between σ/λ^2 and L/λ, respectively

specimens listed in Table 1 and described fully in our earlier study (Lee and Demer 2014).

In this wavelength-normalized form, the TS_m, <TS_b>, and < TS_c > values of cuttlebone are comparable between frequencies:

$$\sigma_p/\lambda^2 = 0.086180\left(L_b/\lambda\right)^{2.977566} \quad (r^2 = 0.88,\ N = 38,\ P < 0.01) \tag{7}$$

for TS_m,

$$\sigma_b/\lambda^2 = 0.069401\left(L_b/\lambda\right)^{2.486144} \quad (r^2 = 0.85,\ N = 38,\ P < 0.01) \tag{8}$$

for < TS_b>, and

$$\sigma_c/\lambda^2 = 0.068449\left(L_c/\lambda\right)^{2.461958} \quad (r^2 = 0.85,\ N = 38,\ P < 0.01) \tag{9}$$

for < TS_c>, where σ_p, σ_b, and σ_c are scattering cross-sectional areas (m^2) corresponding to the TS_m and < TS_b > of cuttlebone and the < TS_c > of cuttlefish, respectively.

Using Eq. (4), the predicted *TS*'s of an individual specimen of cuttlebone and cuttlefish are indicated by:

$$TS_p = 29.78\log_{10}L_b - 9.78\log_{10}\lambda - 21.64 \tag{10}$$

for the predicted value (TS_p) of TS_m,

$$TS_b = 24.86\log_{10}L_b - 4.86\log_{10}\lambda - 22.58 \tag{11}$$

for the predicted value (TS_b) of < TS_b>, and

$$TS_c = 24.62\log_{10}L_c - 4.62\log_{10}\lambda - 22.64 \tag{12}$$

for the predicted value (TS_c) of < TS_c>, where L_b and L_c are the length of cuttlebone (m) and the mantle length of cuttlefish (m), respectively and λ is the wavelength (m).

The mean TS_m values were −28.45 dB at 70 kHz and −25.59 dB at 120 kHz, respectively. These mean TS_m values were 0.09 dB at 70 kHz and 0.71 dB at 120 kHz higher than those predicted by Eq. (10). The mean < TS_b > values were −33.60 dB at 70 kHz and −32.24 dB at 120 kHz. These mean < TS_b > values were 0.11 dB at 70 kHz and 0.33 dB at 120 kHz higher than those predicted by Eq. (11). The differences between the mean TS_m and the mean < TS_b > were 5.14 dB at 70 kHz and 6.65 dB at 120 kHz. The mean < TS_c > values were −33.41 dB at 70 kHz and −32.20 dB at 120 kHz. These mean < TS_c > values were 0.23 dB at 70 kHz and 0.35 dB at 120 kHz higher than that predicted by Eq. (12). Furthermore, for 70 and 120 kHz combined, the mean < TS_c > value was −32.86 dB, 0.11 dB higher than the mean < TS_b > value (−32.87 dB). On the other hand, the mean < TS_c >

predicted by Eq. (12) was −33.06 dB, 0.04 dB higher than the mean $< TS_b >$ predicted by Eq. (11) (−33.10 dB).

Accordingly, the contribution of cuttlebone to cuttlefish *TS* determined by the predicted results was slightly larger than that by the measured results. These results suggest that the cuttlebone is fully responsible for the *TS* of cuttlefish and the contribution is estimated to be more than 99 % of the total echo strength.

Discussion

An example of the 70 and 120 kHz echograms recorded as a function of tilt angle, as the cuttlebone is rotated from the spine-on aspect (−90°) toward the broadside incidence of the dorsal surface in the pitch plane, is shown in Fig. 5. At spine-on and head-on aspects, there was very weak scattering, and as the cuttlebone was approached from the spine-on aspect toward the broadside orientation, the scattering gradually increased. These angular and frequency dependences of acoustic scattering may allow the cuttlefish to be distinguishable from other fish species, which may be expected to have different responses at these frequencies. In particular, the angular dependence on the backscattering in the dorsal plane of the cuttlebone must be accounted for in relation to the improvement of the fish-sizing accuracy of split-beam echo sounders operating at these frequencies. It is also important to note that the tilt-angle dependence of the echo response in Fig. 6 is extremely complex due to the constructive and destructive interference effects of the backscattering signals generated by internal cuttlebone chambers.

In our previous study (Lee and Demer 2014), the orientation for freely swimming cuttlefish was slightly angled head-down relative to the medial axis of the cuttlefish. The strongest backscattering in Fig. 6 was predicted to occur when the cuttlebone surface closest to the sound source is orthogonal to the transducer. However, because of the complexity of the chamber structure, density and curvature of the dorsal surface, the strong echo amplitudes in the echograms for 70 and 120 kHz occurred at slightly head-up aspects (positive tilt-angles).

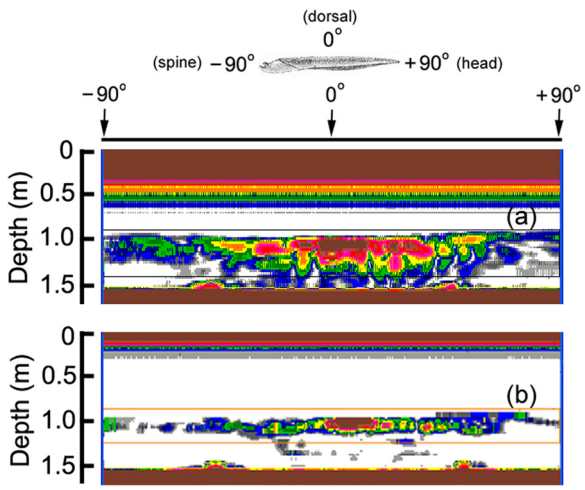

Fig. 6 Comparison of the echograms showing the dependence of echo amplitude on the dorsal orientation of cuttlebone at 70 (**a**) and 120 kHz (**b**). The echogram was recorded as a function of the tilt angle of cuttlebone with significant responses at spine (posterior, −90°), dorsal (0°) and head (anterior, +90°) orientations

The measured *TS* functions, interpolated at 1° intervals, for 70 and 120 kHz are shown in Figs. 7 and 8, respectively; the tilt-averaged *TS* functions for all 19 cuttlebones were overlaid on the plot. In Figs. 7 and 8, a positive tilt angle indicates a head-up posture and a negative tilt angle indicates a head-down posture. The strongest responses were observed at slightly head-up aspects between 1° and 14° at 70 kHz and between 2° and 10° at 120 kHz, and weak responses of approximately −60 dB were observed near the spine-on (−90° aspect) and head-on (+90° aspect) orientations.

For each cuttlebone, these measured *TS* functions were used to calculate the mean *TS* over the range $[<\theta> -3\ S_\theta,\ <\theta> +3\ S_\theta]$ from head-down to head-up orientations by Foote's method (Foote 1980a, 1980b; Pena and Foote 2008). A comparison of the tilt-averaged *TS* functions of cuttlebone at 70 and 120 kHz is shown in Fig. 9. The tilt-averaged *TS* function for 120 kHz showed a strong directivity pattern with higher, narrower peaks and deeper nulls than for 70 kHz, and these *TS* patterns were essentially unimodal with the dominant peaks at slightly positive aspects; the tails in the anterior and posterior orientations extended down to ~60 dB. It appeared that the tilt-averaged *TS* function for 120 kHz exhibited a wider pattern near the peak than at 70 kHz (Fig. 9), but the broadening was due to the overlapping of *TS* patterns with different tilt angles for the peak positions (Figs. 7 and 8). The peak *TS* values in the tilt-averaged *TS* functions were −29.6 dB at a tilt angle of +5° for 70 kHz and −27.5 dB at a tilt angle of +3° for 120 kHz, respectively and the peak *TS* at 120 kHz was 2.1 dB higher that at 70 kHz.

Cuttlebone is bilaterally symmetrical in shape and derived from the juxtaposition of four parts: the outer cone, inner cone, phragmocone and spine. The dorsal surface of cuttlebone is evenly convex in outline but the anterior, median and posterior parts have slightly different curvatures (Neige 2003). Due to these morphological characteristics of cuttlebone, the dependence on the orientation of the cuttlebone *TS* is sensitive to the incidence direction (Figs. 7 and 8).

A comparison of the mean *TS* of cuttlefish with the mean *TS* of cuttlebone is shown in Fig. 10. A comparison of the measured and predicted contributions of cuttlebone to cuttlefish *TS* is shown in Table 3. In

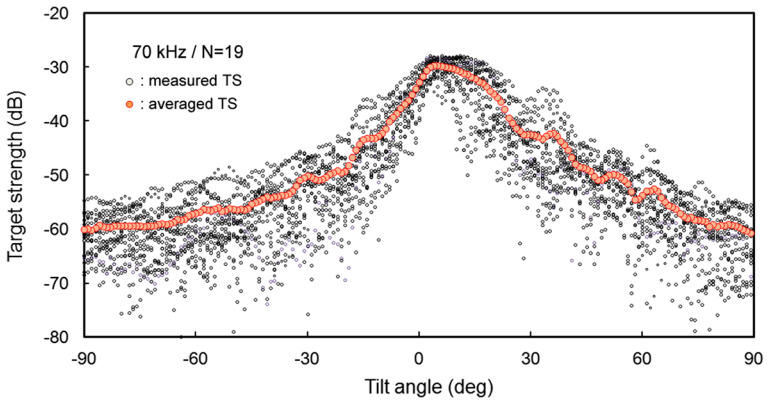

Fig. 7 *TS* functions (*open circle*) for all 19 cuttlebone measured as a function of tilt angle over the angle range [−90°, 90°] from head-down to head-up orientations of the dorsal plane at 70 kHz. The tilt-averaged *TS* function (*solid circle*) was overlaid on the plot

Table 3, the contributions are indicated as the differences between the mean *TS* values that are described within the 95 % confidence limits. In Fig. 10 and Table 3, the mean *TS* values measured using the combined dataset of all 38 specimens for 70 and 120 kHz were −32.76 dB for cuttlefish and −32.87 dB for cuttlebone; i.e., the mean *TS* of cuttlefish was 0.11 dB higher than that of cuttlebone. On the other hand, the mean *TS* values predicted by regressions of the combined dataset of all 38 specimens for 70 and 120 kHz were −33.06 dB for cuttlefish and −33.10 dB for cuttlebone; i.e., the mean *TS* of cuttlefish was 0.04 dB higher than that of cuttlebone. Accordingly, the contribution of cuttlebone to cuttlefish *TS* in the predicted results was slightly larger than in the measured results (Table 3). Furthermore, the measured mean *TS* values of cuttlefish and cuttlebone for a single frequency of 70 kHz were −33.41 and −33.60 dB, respectively; a 0.19 dB difference. The measured mean *TS* values of cuttlefish and cuttlebone at a single frequency of 120 kHz were −33.41 and −33.60 dB, respectively; a 0.19 dB difference. That is, the contribution of cuttlebone at 120 kHz was 0.15 dB higher than at 70 kHz (Table 3). On the other hand, the predicted mean *TS* values of cuttlefish and cuttlebone at a single frequency of 70 kHz were −33.63 and −33.71 dB, respectively; a 0.08 dB difference. The predicted mean *TS* values of cuttlefish and cuttlebone at a single frequency of 120 kHz were −32.55 and −32.60 dB, respectively, a 0.02 dB difference. That is, the contribution of cuttlebone at 120 kHz was 0.06 dB higher than at 70 kHz (Table 3).

The slopes of the regressions for a single frequency in this study were estimated to be 22.03 [95 % confidence interval (CI), 22.03 ± 13.87, $P < 0.01$] at 70 kHz and 28.53 [95 % CI, 28.53 ± 26.29, $P < 0.05$] at 120 kHz [Eqs. (5) and (6)]. These results suggest that the mean *TS* of cuttlebone varies with approximately the square power of the length at 70 and 120 kHz. The intercept [95 % CI,

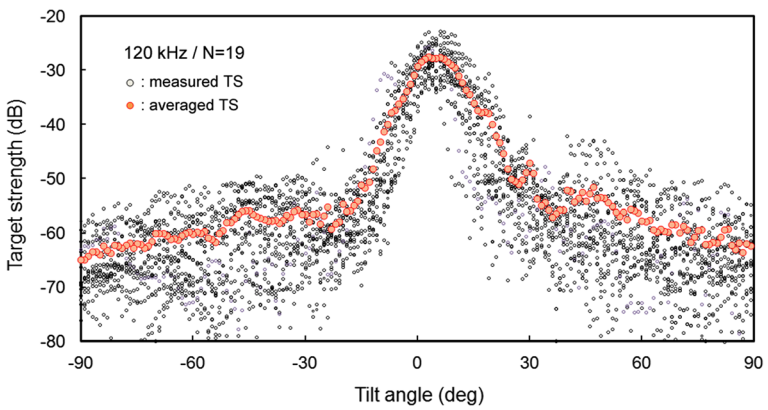

Fig. 8 *TS* functions (*open circle*) for all 19 cuttlebone measured as a function of tilt angle over the angle range [−90°, 90°] from head-down to head-up orientations of the dorsal plane at 120 kHz. The tilt-averaged *TS* function (*solid circle*) was overlaid on the plot

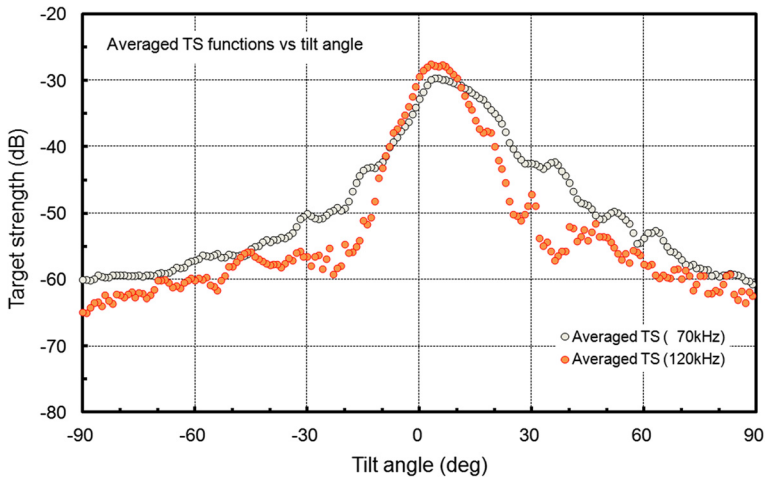

Fig. 9 Comparison of the tilt-averaged *TS* functions of cuttlebone obtained at 70 (*open circle*) and 120 kHz (*solid circle*)

−60.72 ± 17.00 dB, $P < 0.01$] of the regression line at 70 kHz was 6.83 dB higher than at 120 kHz [95 % CI, −67.55 ± 32.21 dB, $P < 0.01$].

According to Simmonds and MacLennan (2005), the slope (m) and intercept (b) of cuttlefish vary widely versus fish species and commonly have values between 18 and 30 and 60 and 80, respectively. The slope and intercept in this study were within these ranges, although the determination coefficient (r^2) indicated relatively low values of $r^2 = 0.40$ at 70 kHz and $r^2 = 0.24$ at 120 kHz. Compared to our earlier study (Lee and Demer 2014), the slopes for cuttlebone were 2.64 at 70 kHz and 12.06

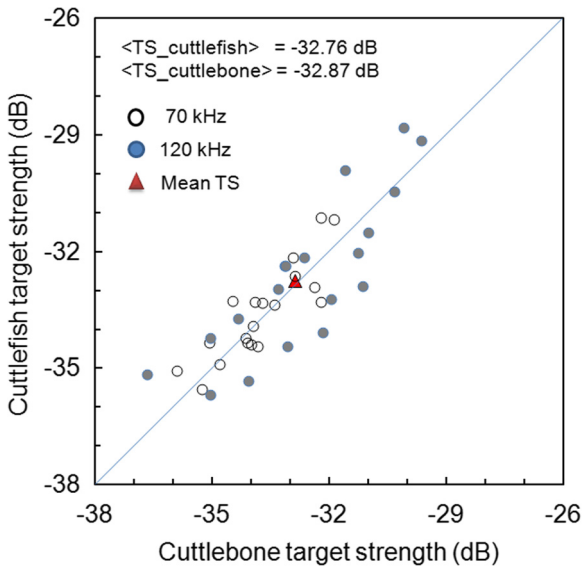

Fig. 10 Relationship between the measured *TS* values for all 38 specimen of cuttlebone and cuttlefish at 70 (*open circle*) and 120 kHz (*solid circle*). Comparison of the mean *TS* ($<TS_c>$) of cuttlefish with the mean *TS* ($<TS_b>$) of cuttlebone was indicated as a solid triangle. Solid line indicates a reference line for comparison

at 120 kHz, lower than those of cuttlefish, and the intercepts for cuttlebone were 3.31 dB at 70 kHz and 15.41 dB at 120 kHz, higher than those of cuttlefish.

The chi-squared test of independence (CSTI, 99 % confidence level) for the TS_m and the $< TS_b >$ values at 70 and 120 kHz showed that the TS_m and the $< TS_b >$ values of cuttlebone at these two frequencies were independent ($P > 0.01$). Accordingly, to compare the TS_m and the $< TS_b >$ values measured at multiple frequencies, a non-dimensional representation may be used (McClatchie et al. 1996; McClatchie et al. 2003, this study). In this study, the 38 wavelength-normalized TS_m and $< TS_b >$ values measured at two frequencies from 19 cuttlebones were compared and showed length-dependent scattering [e.g., Eqs. (10), (11) and (12)]. This formulation allowed twice the number of measurements (38 vs. 19) to be combined in the regression (Love 1969, 1971), which resulted in a considerably better fit [$r^2 = 0.88$ in Eq. (10), $r^2 = 0.85$ in Eq. (11), and $r^2 = 0.85$ in Eq. (12)] (Fig. 5). The fitted coefficient a, b and c values for the regressions of Eqs. (4) and (11) were 24.86 [95 % CI, 24.86 ± 3.57, $P < 0.01$], −4.86 [95 % CI, −4.86 ± 3.57, $P < 0.01$], and −22.58 [95 % CI, −22.58 ± 3.64, $P < 0.01$], respectively. In Fig. 5, the regression of the maximum *TS* (TS_m), which is within the 95 % confidence limit, was ~5 dB higher than that of mean *TS* ($<TS_b>$). Furthermore, at both frequencies, the contributions of the measured results were similar to those of the predicted results (Table 3). It is important to note that if the truncated limit of the tilt-angle distribution in the averaging operation by Foote's method (Foote 1980a, 1980b; Pena and Foote 2008) is controlled, the contribution may be altered to some extent.

The *TS* of cuttlefish is expected to be markedly less depth-dependent than that of swimbladder fish because the buoyancy mechanism of cuttlebone, unlike the fish swimbladder, is almost independent of depth during

Table 3 Comparison of the measured and predicted contributions of cuttlebone on the cuttlefish *TS* at 70 and 120 kHz. The contributions are indicated as the differences between the mean *TS* values that are described within the 95 % confidence limits

Frequency (kHz)	Measured results			Predicted results		
	Cuttlefish (dB)	Cuttlebone TS (dB)	Diff. (dB)	Cuttlefish TS (dB)	Cuttlebone TS (dB)	Diff. (dB)
70	−33.41	−33.60	0.19	−33.63	−33.71	0.08
120	−32.20	−32.24	0.04	−32.55	−32.60	0.02
mean	−32.76	−32.87	0.11	−33.06	−33.10	0.04

vertical movements (Denton and Gilpin-Brown 1961; Denton et al. 1961; Denton and Taylor 1964). Knudsen and Gjelland (2004) reported that at least some coregonid species are capable of filling the swimbladder without access to the surface during the diel vertical migration and that *TS* did not decrease with depth. This swimbladder volume compensation in coregonids is compared to buoyancy regulation by the cuttlebone in cuttlefish. Generally, the change in the surface area of the swimbladder caused by the change in swimbladder volume affects *TS*, but because the dorsal surface of cuttlebone is unaffected by depth, the depth effect of cuttlebone on cuttlefish *TS* is not expected to be affected like the swimbladder of fish. Instead of having a flexible swimbladder like a fish, cuttlefish have a cuttlebone, which has a rigid structure, for buoyancy control. The cuttlebone is divided by many thin, chitinous partitions, which separate gas-filled anterior chambers and fluid-filled posterior chambers of approximately periodic microstructure (Denton and Gilpin-Brown 1961; Denton et al. 1961; Denton and Taylor 1964; Neige 2003; Cadman et al. 2010a, 2010b; Chen et al. 2011). Unlike the swim bladder of fish, cuttlebone is unpressurized, so its volume is not altered markedly as the animal changes depth (Denton and Gilpin-Brown 1961; Denton et al. 1961; Denton and Taylor 1964), and no adjustments to the buoyancy system are necessary during vertical movements (Sherrard 2000).

Generally, the fish *TS* is proportional to the difference in density between the insonified fish target and the surrounding water (Simmonds and MacLennan 2005), and the main source of backscatter is expected to be proportional to the size of the swimbladder, which accounts for at least 90 % of echo energy (Foote 1980a, 1980b, 1985; Foote and Ona 1985). The impedance of gas-filled organs, such as the swimbladder and cuttlebone, differs considerably from that of seawater and other fish tissues, and the scattering contribution of cuttlebone is comparable to that of an air-filled swimbladder. However, in cuttlefish, the problems of pressure changes are avoided by enclosing the gas in the cuttlebone, the volume of which is unaffected by changes in depth and which contains many chambers, some filled with gas and some with liquid. The overall density of the cuttlebone varies between ~0.5 and 0.7, and is controlled by regulating its liquid content (Denton and Gilpin-Brown 1961; Denton et al. 1961; Denton and Taylor 1964). Accordingly, the acoustic scattering by cuttlefish is expected to fluctuate in proportion with changes in the overall density of cuttlebone. Madsen et al. (2007) reported that the muscular mantle and fins of the common squid are the dominant scatterers, and that the hard parts—such as beak, eyes and pen—contribute little to the *TS* of squid, at least for frequencies representative of the clicks of most teutophageous toothed whales. This suggests that the acoustic interference of the muscular mantle, fins and cuttlebone in freely swimming cuttlefish are complexly generated based on frequency.

In this study, the *TS* of cuttlebone was measured and analyzed as a function of length only; however, the *TS* may actually be more sensitive to the dorsal surface area (or volume) of cuttlebone rather than the length. Based on a comparison of the *TS-L* relationships for the corresponding cuttlebone and live cuttlefish for 19 specimens, the contribution of cuttlebone to the backscattering echo strength of cuttlefish was estimated to be at least 99 %. Moreover, the cuttlebone volume (or surface area) may have a greater influence on cuttlefish *TS* than the length, because the proportion of cuttlebone volume as a fraction of the total body volume of cuttlefish (~9.3 %) is almost twofold that of the swimbladder of fish (~5 %) (Denton and Gilpin-Brown 1961; Denton et al. 1961; Denton and Taylor 1964). The relationship between cuttlebone volume and cuttlefish *TS* may be complicated by the complex microstructure of the gas-filled internal shell of the cuttlebone. However, the effects of the morphological and material parameters of cuttlebone—such as length, width, height, density change and curvature of the dorsal surface—must be analyzed to quantitatively estimate the influence of cuttlebone on cuttlefish *TS*. This will be the subject of a future study.

Conclusions

The mean *TS* values of cuttlebone were 0.19 and 0.04 dB lower than those of cuttlefish at 70 and 120 kHz, respectively. The contribution of cuttlebone to the cuttlefish *TS* determined by the measured results was slightly greater than that by the predicted results. From these results, we concluded that cuttlebone is responsible for the *TS* of

cuttlefish, and the contribution is estimated to be at least 99 % of the total echo strength.

Competing interests
The author declares that he has no competing interests.

Author's contribution
DL carried out the experiment, wrote the manuscripts and performed the data analysis. The author approved the final version of the manuscript.

Acknowledgments
This work was supported by a Research Grant of Pukyong National University (2015 year).

Received: 18 March 2016 Accepted: 1 April 2016
Published online: 12 April 2016

References
Benoit-Bird KJ, Gilly WF, Au WWL, Mate B. Controlled and *in situ* target s strengths of the jumbo squid *Dosidicus gigas* and identification of potential acoustic scattering sources. J Acoust Soc Am. 2008;123:1318–28.
Cadman J, Chen Y, Zhou S, Li Q. Creating biomaterials inspired by the microstructure of cuttlebone. Mater Sci Forum. 2010a;654:2229–32.
Cadman J, Zhou S, Chen Y, Li W, Appleyard R, Li Q. Characterization of cuttlebone for a biomimetic design of cellular structures. Acta Mech Sin. 2010b;26:27–35.
Chen Y, Cadman J, Zhou S, Li Q. Computer-aided design and fabrication of bio-mimetic materials and scaffold micro-structures. Adv Mater Res. 2011;213:628–32.
Conti SG, Demer DA. Wide-bandwidth acoustical characterization of anchovy and sardine from reverberation measurements in an echoic tank. ICES J Mar Sci. 2003;60:617–24.
Demer DA, Martin LV. Zooplankton target strength: Volumetric or areal depenpence? J Acoust Soc Am. 1995;98:1111–8.
Denton EJ, Gilpin-Brown JB. The buoyancy of the cuttlefish, Sepia Officinalis (L.). J Mar Bio Ass UK. 1961;41:319–42.
Denton EJ, Taylor DW. The composition of gas in the chambers of the cuttlebone of *Sepia Officinalis*. J Mar Bio Ass UK. 1964;44:203–7.
Denton EJ, Gilpin-Brown JB, Howarth JV. The osmotic mechanism of the cuttlebone. J Mar Bio Ass UK. 1961;41:351–64.
Fnney JL, Robertson GN, McGee CAS, Smith FM, Croll RP. Structure and autonomic innervations of the swim bladder in the zebrafish (Danio rerio). J Comp Neurol. 2006;495:587–606.
Foote KG. Averaging of fish targets strength functions. J Acoust Soc Am. 1980a; 67:504–15.
Foote KG. The importance of the swimbladder in acoustic scattering by fish: A comparison of gadoid and mackerel target strengths. J Acoust Soc Am. 1980b;67:2084–9.
Foote KG. Rather-high-frequency sound scattering by swimbladdered fish. J Acoust Soc Am. 1985;78:688–700.
Foote KG. Fish target strengths for use in echo integrator surveys. J Acoust Soc Am. 1987;82:981–7.
Foote KG. Range compensation for backscattering measurements in the difference frequency nearfield of a parametric sonar. J Acoust Soc Am. 2012; 131:3698–709.
Foote KG, Ona E. Swimbladder cross sections and acoustic target strengths of 13 pollack and 2 saithe. FiskDir Skr Ser HavUnders. 1985;18:1–57.
Goddard GC, Welsby VG. The acoustic target strength of live fish. J Cons Int Explor Mer. 1986;42:197–211.
Horne JK. Acoustic ontogeny of a teleost. J Fish Biol. 2008;73:1444–63.
Imaizumi T, Furusawa M, Akamatsu T, Nishimori Y. Measuring the target strength spectra of fish using dolphin-like short broadband sonar signals. J Acoust Soc Am. 2008;124:3440–9.
Kang D, Mukai T, Iida K, Hwang DJ, Myoung JK. The influence of tilt angle on the acoustic target strength of the Japanese common squid (*Todarodes pacificus*). ICES J Mar Sci. 2005;62:779–89.
Knudsen FR, Gjelland KØ. Hydroacoustic observations indicating swimbladder volume compensation during the diel vertical migration in coregonids (*Coregonus lavaretus* and *Coregonus albula*). Fish Res. 2004;66:337–41.
Lee DJ. Target strength measurements of black rockfish, goldeye rockfish and black scraper using a 70-kHz split beam echo sounder (in Japanese with English abstract). Nippon Suisan Gakkaishi. 2006;72:644–50.
Lee DJ, Demer DA. Target strength measurements of live golden cuttlefish (*Sepia esculenta*) at 70 and 120 kHz. Fish Aquat Sci. 2014;17:361–7.
Love RH. An empirical equation for the determination of the maximum side-aspect target strength of an individual fish. Naval Oceanographic Office. AD849034. 1969. p. 1–17.
Love RH. Measurements of fish target strength: a review. Fish Bull. 1971;69:703–15.
Madsen PT, Wilson M, Johnson M, Hanlon RT, Bocconcelli A, Aguilar de Soto N, et al. Clicking for calamari: toothed whales can echolocate squid *Loligo pealeii*. Aquat Biol. 2007;1:141–50.
McClatchie S, Alsop J, Coombs RF. A re-evaluation of relationships between fish size, acoustic frequency, and target strength. ICES J Mar Sci. 1996;53:780–91.
McClatchie S, McCauley GJ, Coombs RF. A requiem for the use of 20 $\log_{10}$ Length for acoustic target strength with special reference to deep-sea fishes. ICES J Mar Sci. 2003;60:419–28.
Midtvedt D, Sobko T, Midtvedt T. Nitric oxide (NO) gas present in the swim bladder of cod (*Gadus morhua*). Microb Ecol Health Dis. 2007;19:150–2.
Neige P. Combining disparity with diversity to study the biogeographic pattern of sepiida. Berliner Paläobiol Abh. 2003;3:189–97.
Pena H, Foote KG. Modelling the target strength of *Trachurus symmetricus murphyi* based on high-resolution swimbladder morphometry using an MRI scanner. ICES J Mar Sci. 2008;65:1751–61.
Sawada K, Uchikawa K, Matsuura T, Sugisaki H, Amakasu K, Abe K. *In situ* and *Ex situ* target strength measurement of mesopelagic lanternfish, *Diaphus theta* (Family mactophidae). J Mar Sci Technol. 2011;19:302–11.
Sherrard KM. Cuttlebone morphology limits habitat depth in eleven species *Sepia* (Cephalopoda: Sepiidae). Biol Bull. 2000;198:404–14.
Simmonds J, MacLennan D. Fisheries Acoustics. Oxford: Blackwell Publishing; 2005.
Sunardi, Yudhana A, Din J, Bidin R, Hassan R. Swimbladder on fish target strength. Telkomnika. 2008;6:139–44.
Webber DM, Aitken JP, O'Dor RK. Costs of locomotion and vertic dynamics of cephalopods and fish. Physiol Biochem Zool. 2000;73:651–62.

Submit your next manuscript to BioMed Central and we will help you at every step:

- We accept pre-submission inquiries
- Our selector tool helps you to find the most relevant journal
- We provide round the clock customer support
- Convenient online submission
- Thorough peer review
- Inclusion in PubMed and all major indexing services
- Maximum visibility for your research

Submit your manuscript at
www.biomedcentral.com/submit

BioMed Central